2-D numerical investigation on load transfer in pile-supported fill platforms subjected to cyclic loading

Zhen Zhang, Guanbao Ye & Fengjuan Tao
Tongji University, China

Jie Han
The University of Kansas, USA.

ABSTRACT: Geosynthetic-Reinforced Pile-Supported (GRPS) fill platforms have been increasingly used as an expedite technique for embankment construction over soft soils. In the past decades, most studies have focused on the behavior of GRPS fill platforms under static loading. However, the GRPS embankments are subjected to traffic loading in service. Some experimental tests also showed that cyclic loading would weaken the load transfer from soil to piles. In this paper, a series of two-dimensional (2-D) numerical analyses were conducted to investigate the load transfer in GRPS embankments under cyclic loading. A uniform cyclic pressure was applied on the embankment surface. The numerical model was first calibrated using a model test available in the literature. After that, the model was used to investigate the influence factors of the thickness of granular fill, the geosynthetic reinforcement, and the load type (static load and cyclic load) on soil arching effect. The numerical results show that the cyclic load weakened the load transfer function of the gravel fill since more load was transferred onto the moveable part and more surface differential settlement took place as compared with those under the static load. However, the geosynthetic reinforcement minimized the effect of the cyclic load on the soil arching, especially under the thin fill condition. A curved soil arch with lower and upper boundaries was identified under a thick fill condition and the critical height of the soil arch was almost identical under both static and cyclic loading conditions. Modified factors for soil arching ratio are proposed to consider the influence of the cyclic load on the soil arching effect.

Keywords: GRPS fill platform; Soft soils; Load transfer; Cyclic load; Numerical analysis

1 INTRODUCTION

Geosynthetic-Reinforced Pile-Supported (GRPS) fill platforms have been increasingly used as an expedite technique for embankment construction over soft soils. This technique involves placement of a granular fill cushion at pile heads to reduce total and differential settlements and enhance load transfer from soil to piles due to soil arching, tensioned membrane, and stress concentration effects (Han and Gabr, 2002). In the past decades, most studies have focused on the behavior of GRPS fill platforms under static loading (Jenck et al., 2009; Iglesia et al., 2011; van Eekelen et al., 2013; Girout et al., 2014). However, when this technique has been adopted to support embankments, backfill materials (including gravel cushion and embankment fill) are subjected to traffic loading in service. Some experimental tests showed that cyclic loading would weaken the load transfer from soil to piles (Heitz et al., 2008; Han et al., 2014). Zhuang and Li (2015) indicated that the stress levels in soil arch were much closer to the critical state under the traffic load than those under the static load. However, Okyay et al. (2013) found that the efficiency of load transfer under cyclic loading was similar to that under monotonic loading based on the centrifugal tests.

Regarding the influence of geosynthetic reinforcement on the performance of GRPS embankments under cyclic loading, Han and Bhandari (2009) numerically demonstrated that the geosynthetic reinforcement could reduce the deformation by 25% as compared to the unreinforced embankment under the cyclic load. van Eekelen et al. (2012) showed that the approach assuming an inverse triangular earth pressure on the geogrid reinforcement gave better agreement with the geogrid strains measured during truck passages.

This paper presents a series of two-dimensional (2-D) numerical analysis to investigate the load transfer characteristics in GRPS embankments under cyclic loading. A uniform cyclic pressure was applied on the embankment surface. The numerical model was first calibrated using the model test reported by Jenck et al. (2014). After that, the influence factors including the thickness of granular fill, the geosynthetic reinforcement, and the load type (static load or cyclic load) on the load transfer behavior were investigated. Modified factors for soil arching ratio (SAR) were proposed to consider the influence of the cyclic load on the soil arching effect.

2 NUMERICAL MODELING

2.1 *Model configuration*

Jenck et al. (2014) conducted a series of model tests to investigate the soil arching effect in a granular soil subjected to cyclic loading, which was adopted for the numerical analysis in this study. Fig. 1 shows the setup of the model test. A brief introduction is presented herein. The three sides of the model box were made of plywood and the front side was made of Plexiglas allowing the observation and photogrammetry of the granular fill during the test. The model box was reinforced by steel frames to minimize deformations. The base of the box had a length of 1 m and a width of 0.4 m. The moveable part with a dimension of 0.2m ×0.4m was made of a foam element placed between two wooden plates. This moveable part was used to simulate soft soil between piles. The granular fill of 0.1 m thick was placed on the top of the foam (moveable part) and the stationary part. The displacement of the moveable base was measured by a displacement transducer (LVDT) and the load carried by the moveable base was measured by a load cell.

The cyclic load was applied by filling water into the water tank placed on the granular fill using a water pump. The maximum uniform vertical stress of 8 kPa on the granular fill surface and the loading-unloading cycle was 80 min. The cyclic loading is illustrated in Fig. 2. The granular fill had a peak friction angle of 48° and a residual friction angle of 40° determined by drained triaxial tests. The behavior of the foam element made of polyurethane was almost elastic during the loading-unloading cycles.

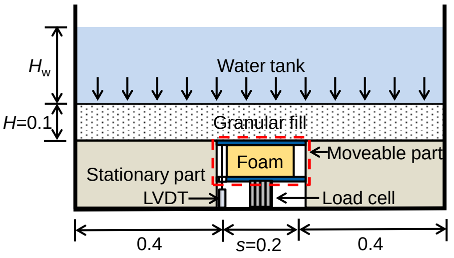

Unit: m

Figure 1. Schematic view of the setup under cyclic loading (modified from Jenck et al. 2014)

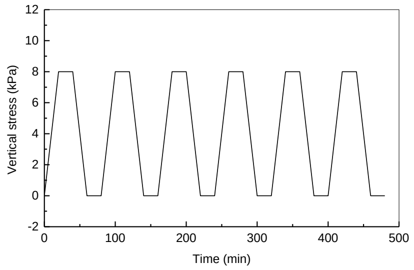

Figure 2. Loading-unloading cycles with time

The two-dimensional (2-D) finite element program ABAQUS was used to investigate the arching effect in the granular fill under cyclic loading. The geometry of the numerical model was established based on the model test conducted by Jenck et al. (2014). Two conditions were considered in the numerical models: (a) thin gravel fill (0.1 m thick); (b) thick gravel fill (0.5 m thick). The corresponding ratios of the granular fill thickness to the stationary part clear spacing were 0.5 and 2.5, respectively. Fig. 3 shows the finite element meshes with the fill thickness of 0.1 m. The numerical model with the fill thickness of 0.5 m had an identical configuration except for the fill thickness. For the model calibration, the experimental test was simulated based on the numerical model with the fill thickness of 0.1 m, and the numerical results are compared with the experimental results later.

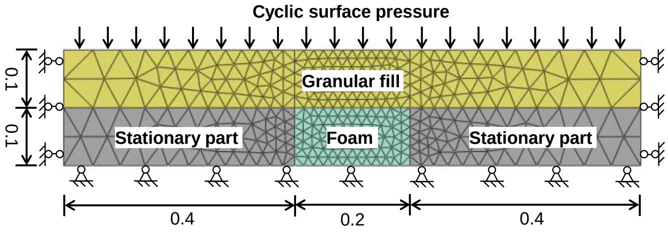

Figure 3. Two-dimensional numerical model (unit: m)

2.2 *Material properties and boundary conditions*

The foam and the stationary part were modeled as linearly elastic materials. The fill was modeled as an elastic-plastic material with the modified Drucker-Prager constitutive model. The modified Drucker-Prager model is intended for geological materials that exhibit pressure-dependent yield. The cap hardening behavior was considered using the function related to the cap pressure (p_c) and the cap plastic volumetric strain (e^p),

$$\mathrm{d}p_\mathrm{c} = \frac{1+R}{R} K_{ref}^{iso} \left(\frac{p'}{p_{ref}} \right)^m \mathrm{d}e^p \tag{1}$$

where R is the cap eccentricity; K_{ref}^{iso} is the slope of the laboratory curve for effective mean principal stress (p') versus void ratio (e) at the reference effective pressure (p_{ref}), and m is a constant (m=0.4). Rayleigh damping was used in the analysis and the Rayleigh damping factor for stiffness proportional damping (β_R) was determined based on a natural frequency of oscillation and a fraction of critical damping. Table 1 shows the material properties used in the numerical modeling.

To investigate the effect of geoysnthetic reinforcement on the arching effect, a single layer of geosynthetic was placed in the gravel fill and at 10 mm above the stationary part. The geosynthetic was simulated using a membrane element with tensile stiffness J=1200 kN/m. The embedded element technique was introduced to model the interaction between the geosynthetic and the gravel fill.

Table 1. Material properties used in FEM analysis

Material	**Properties**
Gravel	γ = 18 kN/m^3, v = 0.3, E = 20 MPa, d=10Pa, ϕ = 52°, R=0.67, $\varepsilon_{\mathrm{vol}}^{in}$ =0.00063, k=1, β_R=0.00043
Foam	v = 0.2, E = 500 kPa
Stationary part	v = 0.2, E = 1 MPa

Note: γ = unit weight, v = Poisson's ratio, E = elastic modulus, d = material cohesion, ϕ = friction angle in the cap plasticity model, R = cap eccentricity, $\varepsilon_{\mathrm{vol}}^{in}$ = initial yield surface position, k = flow stress ratio, β_R = Rayleigh damping factor for stiffness proportional damping.

The dynamic implicit method incorporated in the ABAQUS program was implemented to conduct the dynamic analysis. The cyclic load induced by water pumping was simulated by adding the equivalent cyclic surface pressure on the surface of the granular fill. For model calibration, the cyclic load illustrated in Fig. 2 was simulated, while for the investigation, the cyclic load was modeled as a sine function with maximum and minimum pressures of 8 kPa and 0 kPa and a frequency of 1 Hz. The bottom boundary of the numerical model was fixed in both horizontal and vertical directions and the two side boundaries were fixed in the horizontal direction but allowed to move freely in the vertical direction.

3 MODEL VALIDATION

The vertical pressure and the deflection of the foam were measured during the test. Fig. 4 shows the comparisons between the numerical results and the test results. It can be seen that the measured vertical pressures and settlements on the foam agreed well with the numerical results. The maximum vertical pressures, the maximum settlements, and the accumulated (permanent) settlements increased with cycles, which indicate that the behavior of the load transfer platform under cyclic loading is different that under static loading.

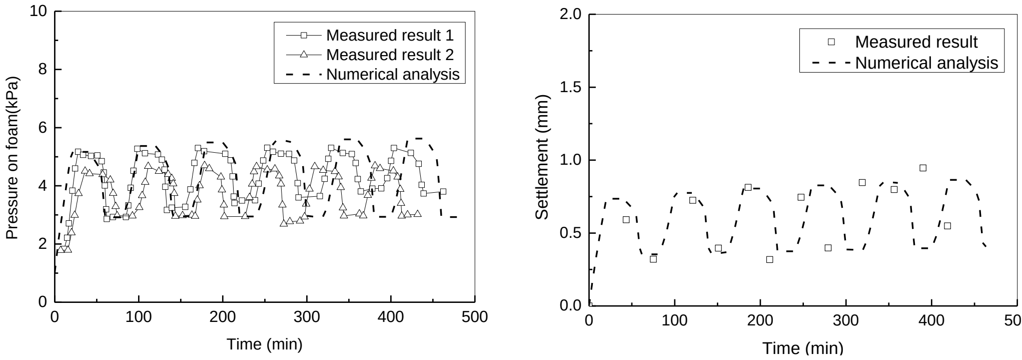

(a) (b)

Figure 4. Comparison between numerical results and measured data: (a) earth pressures on foam; (b) settlement on foam

4 RESULTS AND DISCUSSION

4.1 *Effect on surface settlement*

Fig. 5 presents the variation of the central settlement on the fill surface with load cycles and the results for static loads for comparison purposes. Under the thin fill condition, the total settlements under cyclic loading increased gradually with the load cycles and exceeded the settlement under static loading. When the geosynthetic was included, the total settlement and the accumulated settlement were reduced. However, under the thick fill condition, the total settlements for the model without geosynthetic subjected to cyclic loading were almost the same as those under static loading. The geosynthetic reduced the settlement slightly.

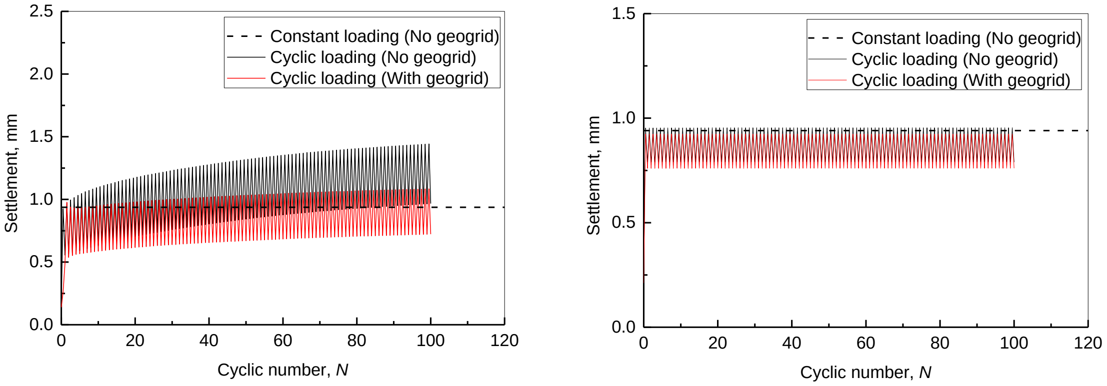

(a) (b)

Figure 5. Variation of settlement on the center of fill surface with loading cycles: (a) thin fill (H/s=0.5); (b) thick fill (H/s=2.5)

Fig. 6 compares the profiles of the differential settlement on the fill surface after 100 cycles. It can be clearly seen that the differential settlements under cyclic loading were larger than those under static loading under both the thin and thick fill conditions. The inclusion of geosynthetic reinforcement was beneficial in reducing the differential settlement on the surface. Under the thin fill condition, more differential settlement took place as compared with that under the thick fill. The above analyses indicate that more accumulated deformation would occur under cyclic loading as compared with that under static loading. The thickness of the granular fill and the inclusion of geosynthetic reinforcement reduced the differential settlement under cyclic loading.

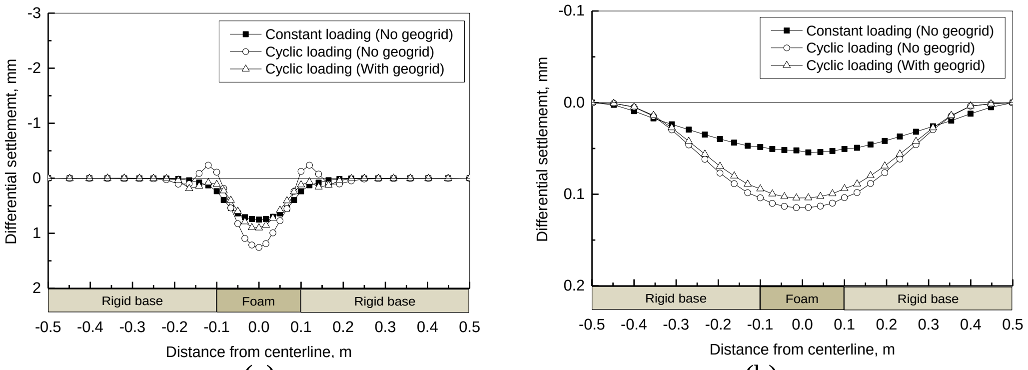

(a) (b)

Figure 6. Differential settlement profile on the fill surface: (a) thin fill (H/s=0.5); (b) thick fill (H/s=2.5)

4.2 *Effect on load transfer*

To explore the arching effect in the granular fill, the vertical stress ratio, defined as the ratio of the vertical stress induced by the granular fill and/or surface surcharge along the centerline of the foam to that along the edge of stationary part at different depth in the fill, is introduced herein. When the complete soil arch is formed in the fill, the vertical stresses in the fill are identical everywhere at the same elevation above the height of soil arch. In other words, the height of complete soil arch can also be determined by the equal vertical stress plane in the fill.

In Fig. 7, the fill height was normalized as the ratio of fill height to clear stationary part spacing. Fig. 7(a) shows that no complete soil arch existed in the thin fill and the vertical stress ratio decreased under cyclic loading. This result indicates that the cyclic load had a significant effect on load transfer when no complete soil arch was formed in the fill. However, under the thick fill condition (see Fig. 7(b), the fill thickness was 2.5 times the clear spacing which was more than enough for the fill to form a complete soil arch. As a result, the profiles of the vertical stress ratio were almost identical under both cyclic and static loading. The critical height of soil arch happened at the height of 1.5 times the clear spacing for all the three cases where the vertical stress ratios became constant (i.e., 1.0).

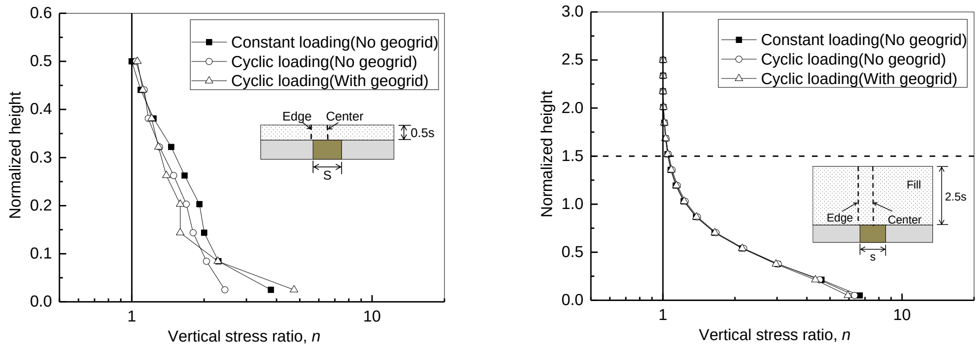

(a) (b)

Figure 7. Vertical stress ratio between the centerline of the foam and the edge of the stationary part at different fill depth after 100 load cycles: (a) thin fill (H/s=0.5); (b) thick fill (H/s=2.5)

To further investigate the role the granular fill played in the embankment system under different load conditions, the soil arching ratio (SAR) and the differential settlement reflection ratio were evaluated. The soil arching ratio is defined as the ratio of the vertical stress on the movable part to the average stress (including the fill weight and the surcharge). The differential settlement reflection ratio is defined as the ratio of the maximum differential settlement on the surface of granular fill to that at the base of granular fill (Blanc et al. 2014). Clearly, a lower soil arching ratio and/or differential settlement reflection ratio indicates that the granular fill (with or without geosynthetic reinforcement) plays a more effective role in the embankment system. Fig. 8 shows that the thick fill significantly reduced the soil arching ratio and the differential settlement reflection ratio. However, the cyclic load weakened the role of the granular fill since more load was transferred onto the moveable part and more surface differential settlement took place as compared with the case under the static load. Under the thin fill condition, the differential settlement reflection ratio under cyclic loading was greater than 1.0 since more accumulated deformations occurred near the shallow region of the granular fill above the edge of the movable part and the profile of the surface settlement as discussed later. Fig. 8 also shows that the geosynthetic reinforcement reduced the differential settlement reflection ratio under dynamic loading, especially under the thin fill condition.

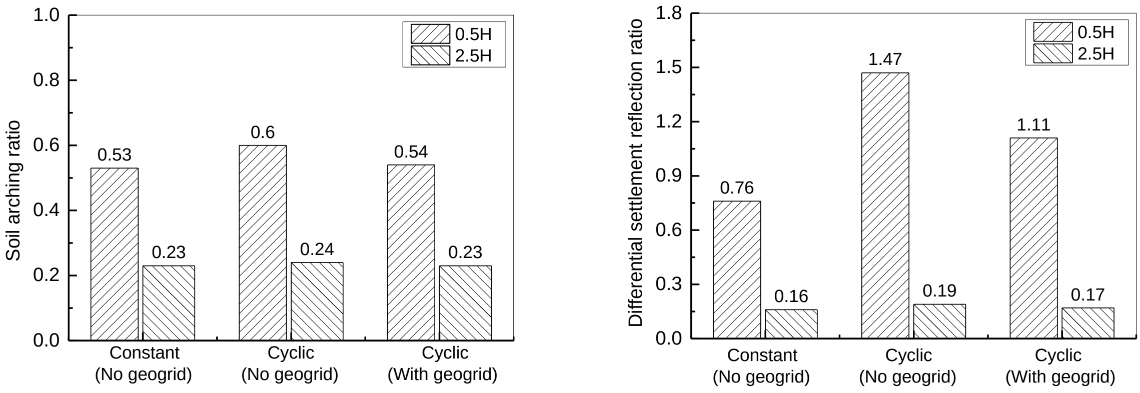

(a) (b)

Figure 8. Degree of load transfer and deformation at 100 load cycles: (a) Soil arching ratio; (b) Differential settlement reflection ratio

4.3 *Effect on soil arch shape*

Iglesia et al. (2013) explained the evolution of soil arching from a curved arch to a triangular arch and ultimately to a trench arch. Different arch models were investigated based on the contours of the vertical stress and the vectors of the maximum principal stresses in the fill in this section.

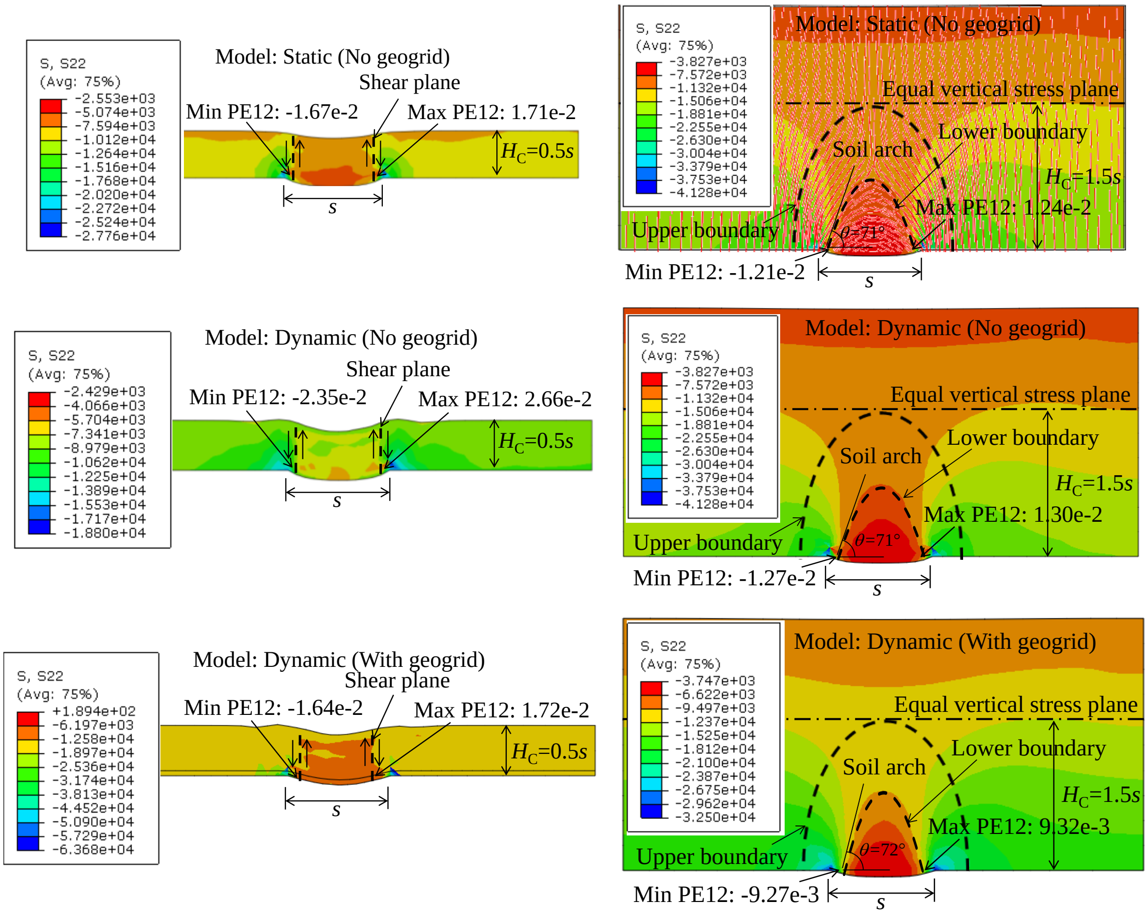

(a) (b)

Figure 9. Contours of vertical stresses at 100 load cycles: (a) thin fill (H/s=0.5); (b) thick fill (H/s=2.5)

Fig. 9 shows that under the thin fill condition, the vertical stresses in the gravel fill above the movable part were lower than those above the stationary part. For this case, the shape of the soil arch was more like the trench arch model proposed by Terzaghi (1943). Under the thick fill condition, the fill was thick enough to form a complete soil arch in a curved shape. Within the curved soil mass were low vertical stresses above the movable part. Based on the distribution of the vertical stress in the fill, a parabolic arch model was used to fit the curved soil mass above the movable part. The boundary of the curved soil mass is referred to as the lower boundary of the soil arch in this paper. The tangential angle θ starting from the base of the soil arch was approximately 71° to 72°, which is consistent to the angle of the slip planes in the Rankine active state (i.e., $45° + \varphi/2 = 69°$). On the other hand, the vertical stresses nearby the edge of the stationary part were higher than those far away from the edge due to the soil arching effect. The equal vertical stress plane developed at the height of about 1.5 times the clear spacing. These two observations were used to determine the base and the crown of the upper boundary of the soil arch. Then following the flows of the vectors of maximum principle stress in the fill (see the upper figure in Fig. 9 (b)), the upper boundary of the soil arch can be obtained which had a shape of approximate semi-ellipse. Since under the thick fill condition the upper boundaries of soil arch were similar, the middle and lower figures in Fig 9(b) exclude the vectors of maximum principle stresses in the fill.

In addition, Fig. 9 includes the maximum plastic shear strains as denoted as PE12. Under both thin and thick fill conditions, the maximum plastic shear strains occurred at the edge of the stationary part. The cyclic load increased the maximum plastic shear strains in the fill while the inclusion of geosynthetic reinforcement could mitigate the dynamic effect on the increased plastic shear strain. Therefore, the inclusion of geosynthetic reinforcement reduced the soil plastic strain under cyclic loading.

4.4 *Modified factor for cyclic load*

Based on the preceding analyses, a modified factor for the soil arching ratio is proposed to consider the influence of cyclic loading on the soil arching effect. This factor is defined as the ratio of the soil arching ratio under cyclic loading to that under static loading. Fig. 10 shows the modified factor for the soil arching ratio with the normalized fill height. Under the condition without geosynthetic, the modified factor for the soil arching ratio decreased with the increase in the fill height, while when the geosynthetic was included, the modified factor for the soil arching ratio was approximately equal to 1.0 irrespective of the fill height. When the normalized height (H/s) was 2.5, the cyclic load almost had no effect on the soil arching ratio. Heitz et al. (2008) proposed a series of curves to consider the influence of the cyclic load on the soil arching effect. Fig. 10 shows that the data points plotted based on the numerical results had a similar tendency as the curves proposed by Heitz et al. (2008). It should be noted that based on Heitz et al. (2008), the soil arching effect also depends on the magnitude and frequency of cyclic load. A further study is needed to verify their results in the future.

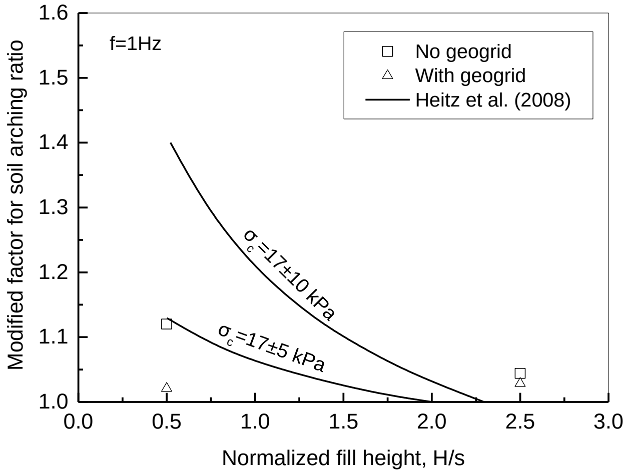

Figure 10. Modified factor for soil arching ratio

5 CONCLUSIONS

A series of 2-D numerical analyses were conducted to investigate the soil arching effect in a granular fill subjected to cyclic loading. The influence of geosynthetic reinforcement on the soil arching effect was considered. Based on the numerical analyses, the following conclusions can be drawn:

1. The cyclic load had a significant effect on load transfer between stationary and moveable parts when no complete soil arch was formed in the fill. The critical height of soil arch was 1.5 times the clear spacing

under the static and cyclic loading conditions when the granular fill had enough thickness to form a complete soil arch.

2. The cyclic load weakened the load transfer function of the granular fill. More load was transferred onto the movable part and more surface differential settlement took place under cyclic loading as compared with those under static loading. Geosynthetic reinforcement minimized the effect of the cyclic load, especially under the thin fill condition.
3. Under the thin fill condition, the soil arch was more like the trench arch model proposed by Terzaghi (1943). Under the thick fill condition, a parabolic soil arch referred to as the lower boundary was formed above the moveable part, while an upper boundary of the soil arch was identified based on the distribution of vertical stresses nearby the edge of the stationary part and the equal vertical stress plane in the fill. The geosynthetic reinforcement reduced the soil plastic strain under cyclic loading.
4. A modified factor was proposed to consider the influence of cyclic loading on the soil arching effect. Under the condition without geosynthetic, the modified factor for the soil arching ratio decreased with the increase in fill height, while when the geosynthetic was included, the modified factor for the soil arching ratio was approximately equal to 1.0 irrespective of fill height. When the normalized height (fill height/clear spacing) was 2.5, the cyclic load had almost no effect on the soil arching ratio.

ACKNOWLEDGMENTS

The authors appreciate the financial support provided by the Natural Science Foundation of China (NSFC) (Grant No. 51478349 & No. 51508408) and the Pujiang Talents Scheme (No. 15PJ1408800) for this research.

REFERENCES

Girout, R., Blanc, M., Dias, D., and Thorel, L. (2014). Numerical analysis of a geosynthetic-reinforced piled load transfer platform-validation on centrifuge test. Geotextiles and Geomembranes, 42(5), 525-539.

Han, G.-X., Gong, Q.-M., & Zhou, S.-H. (2014). Soil arching in a piled embankment under dynamic load. International Journal of Geomechanics, 15(6), 04014094.

Han, J., and Bhandari, A. (2009). Evaluation of Geogrid-Reinforced Pile-Supported Embankments under Cyclic Loading Using Discrete Element Method. U.S.-China Workshop on Ground Improvement Technologies, In Advances in Ground Improvement: Research to Practice in the United States and China, pp.73-82.

Han, J., and Gabr, M. A. (2002). Numerical analysis of geosynthetic-reinforced and pile-supported earth platforms over soft soil. Journal of geotechnical and geoenvironmental engineering, 128(1), 44-53.

Heitz, C., Lüking, J., and Kempfert, H.G. (2008). Geosynthetic Reinforced and Pile supported Embankments under Static and Cyclic Loading. Proceedings of European Geosynthetics Conference Eurogeo 2008, pp. 215-222.

Iglesia, G. R., Einstein, H. H., and Whitman, R. V. (2013). Investigation of soil arching with centrifuge tests. Journal of Geotechnical and Geoenvironmental Engineering, 140(2), 04013005.

Jenck, O., Dias, D., and Kastner, R. (2009). Three-dimensional numerical modeling of a piled embankment. International Journal of Geomechanics, 9(3), 102-112.

Jenck, O., G. Combe, F. Emeriault, and A. De Pasquale. (2014). Arching effect in a granular soil subjected to monotonic or cyclic loading: kinematic analysis. In 8th international conference on physical modelling in geotechnics, Perth, Australia, pp. 14-17.

Okyay, U. S., Dias, D., Thorel, L., and Rault, G. (2013). Centrifuge modeling of a pile-supported granular earth-platform. Journal of Geotechnical and Geoenvironmental Engineering, 140(2), 04013015.

Terzaghi, K. (1943). Theoretical Soil Mechanics. John Wiley and Sons, New York.

van Eekelen, S. J. M., Bezuijen, A., and van Duijnen, P. G. (2012). Does a piled embankment ‘feel’the passage of a heavy truck? Field measurements. In proceedings of the 5th European Geosynthetics Congress EuroGeo, Vol. 5, pp. 162-166.

van Eekelen, S. J. M., Bezuijen, A., and van Tol, A. F. (2013). An analytical model for arching in piled embankments. Geotextiles and Geomembranes, 39, 78-102.

Zhuang, Y., and Li, S. (2015). Three-dimensional finite element analysis of arching in a piled embankment under traffic loading. Arabian Journal of Geosciences, 8(10), 7751-7762.